The metabolic gene HAO2 is downregulated in hepatocellular carcinoma and predicts metastasis and poor survival

The metabolic gene HAO2 is downregulated in hepatocellular carcinoma and predicts metastasis and poor survival

Sandra Mattu[1, †], Francesca Fornari[2, †], Luca Quagliata[3, †], Andrea Perra[1], Maria Maddalena Angioni[1], Annalisa Petrelli[4], Silvia Menegon[4], Andrea Morandi[5], Paola Chiarugi[5], Giovanna Maria Ledda-Columbano[1], Laura Gramantieri[2], Luigi Terracciano[3], Silvia Giordano[4] , Amedeo Columbano[1]

[1] Department of Biomedical Sciences, University of Cagliari, Cagliari, Italy
[2] St.Orsola-Malpighi University Hospital, Bologna, Italy
[3] Institute of Pathology, University Hospital, Basel, Switzerland
[4] University of Torino School of Medicine, Candiolo Cancer Institute-FPO, IRCCS Candiolo (Torino), Italy
[5] Department of Experimental and Biomedical Sciences, University of Firenze, Firenze, Italy
† These authors contributed equally as joint first authors.

Background & Aims

L-2-Hydroxy acid oxidases are flavin mononucleotide-dependent peroxisomal enzymes, responsible for the oxidation of L-2-hydroxy acids to ketoacids, resulting in the formation of hydrogen peroxide. We investigated the role of HAO2, a member of this family, in rat, mouse and human hepatocarcinogenesis.

Methods

We evaluated Hao2 expression by qRT-PCR in the following rodent models of hepatocarcinogenesis: the Resistant-Hepatocyte, the CMD and the chronic DENA rat models, and the TCPOBOP/DENA and TCPOBOP only mouse models. Microarray and qRT-PCR analyses were performed on two cohorts of human hepatocellular carcinoma (HCC) patients. Rat HCC cells were transduced by a Hao2 encoding lentiviral vector and grafted in mice.

Results

Downregulation of Hao2 was observed in all investigated rodent models of hepatocarcinogenesis. Interestingly, Hao2 mRNA levels were also profoundly downregulated in early preneoplastic lesions. Moreover, HAO2 mRNA levels were strongly downregulated in two distinct series of human HCCs, when compared to both normal and cirrhotic peri-tumoral liver. HAO2 levels were inversely correlated with grading, overall survival and metastatic ability. Finally, exogenous expression of Hao2 in rat cells impaired their tumorigenic ability.

Conclusion

Our work identifies for the first time the oncosuppressive role of the metabolic geneHao2. Indeed, its expression is severely decreased in HCC of different species and etiology, and its reintroduction in HCC cells profoundly impairs tumorigenesis. We also demonstrate that dysregulation of HAO2 is a very early event in the development of HCC and it may represent a useful diagnostic and prognostic marker for human HCC.

Abbreviations

2-AAF, 2-acetylaminofluorene;
CAR, constitutive androstane receptor;
CMD, choline devoid-methionine deficient diet;
DENA, diethylnitrosamine;
GAPDH, glyceraldehyde 3-phosphate dehydrogenase;
GSTP, placental glutathione S-transferase;
HAO2, 2-hydroxy acid oxidase-2;
HCC, hepatocellular carcinoma;
KRT-19, cytokeratin-19;
PH,partial hepatectomy;
qRT-PCR, quantitative reverse transcriptase polymerase chain reaction;
ROS, reactive oxygen species;
R-H model, Resistant-Hepatocyte model;
R-H, resistant hepatocellular carcinoma cells;

TCPOBOP, 1,4-Bis-[2-(3,5-dichloropyridyloxy)]benzene

Keywords
Hydroxy acid oxidases; Multistage liver carcinogenesis; HCC; TCPOBOP

Introduction

L-2-Hydroxy acid oxidases are flavin mononucleotide (FMN)-dependent peroxisomal enzymes, which are members of the flavoenzyme family responsible for the oxidation ofL-2-hydroxy acids to ketoacids at the expense of molecular oxygen, resulting in the formation of hydrogen peroxide [1]. In humans, there are three 2-hydroxy acid oxidase genes named HAO1, HAO2, and HAO3 (also known as HAOX1, HAOX2 and HAOX3), which encode peroxisomal proteins with 2-hydroxy acid oxidase activity [1]. All the members of the hydroxy oxidase family are highly conserved; human HAO2 shares ∼50% identity with human HAO1 and 72–74% identity with rodent (rat and mouse) Hao2[2]. HAO2 is predominantly expressed in the liver and kidney, and shows greatest enzymatic activity for long chain 2-hydroxy acid substrates. HAO1 is expressed primarily in the liver and pancreas and shows greatest potency for the two-carbon 2-hydroxy acid substrate glycolic acid, but it is active also on long chain 2-hydroxy fatty acids. HAO3 is expressed primarily in the pancreas and its preferential substrate is 2-hydroxyoctanoate[1].

Since 2-hydroxy acid oxidases are involved in the oxidation of 2-hydroxy fatty acids, they might also contribute to the general pathway of fatty acid α-oxidation [1], as they can oxidize a broad range of 2-hydroxy acids, ranging from glycolate to long chain 2-hydroxy fatty acids such as 2-hydroxypalmitate [3], [4] and [5]. These enzymes utilize a flavin cofactor and convert 2-hydroxy acids to 2-keto acids, with the concomitant reduction of molecular oxygen to hydrogen peroxide. By producing hydrogen peroxide, the reaction catalyzed by members of HAO2 family might contribute to increase the levels of reactive oxygen species (ROS) and, consequently, play a role in cell injury. On the other hand, increased generation of ROS levels might also represent a stimulus for the induction of cell proliferation [6] and [7]. Unfortunately, no data are available on the role of 2-hydroxy acid oxidases in biological processes involving cell death and cell proliferation, such as cancer.

Our recent microarray analysis showing Hao2 downregulation in rat HCC [8] prompted us to investigate a possible role of this gene in HCC development. With this aim, we analysed HAO2 expression in HCCs developed in three different species (mouse, rat and human), and caused by different etiological agents.

Materials and methods

Animal experiments

Male Fischer (F-344) and Wistar rats, female C3H mice and CD-1 nude mice were obtained from Charles River, Milano, Italy. Guidelines for Care and Use of Laboratory Animals were followed during the investigation. All animal procedures were approved by the Ethical Commissions of the Universities of Cagliari, Bologna, Turin and the Italian Ministry of Health.

Rat models

R-H model: Male F-344 rats were injected intraperitoneally with diethylnitrosamine (DENA, Sigma, St. Louis, MO, USA) at the dose of 150 mg/kg body weight. After a 2-week recovery period, rats were fed a diet containing 0.02% 2-acetylaminofluorene (2-AAF, Sigma) for 1 week, followed by a two-thirds partial hepatectomy (PH), and an additional week of 2-AAF diet [9]. The animals were then returned to the basal diet and euthanized at 10 weeks, 10 months or 14 months. The number of GSTP-positive preneoplastic foci was determined as previously described [8].

CMD model: Male F-344 rats were injected intraperitoneally with a single dose of DENA (150 mg/kg body weight) and fed a choline devoid-methionine deficient diet [10]. Animals were euthanized at 10 weeks, 4 months or 13 months after DENA treatment.

Chronic DENA administration model: DENA was given in the drinking water (100 mg/L) for 8 weeks [11] to male Wistar rats. Two weeks after the end of carcinogen administration, animals were monitored weekly by ultrasound imaging (Esaote) for HCC development and euthanized 1 to 2 months later.

Mouse models

Female C3H mice were injected intraperitoneally with DENA at the dose of 90 mg/kg body weight. After a 1-week recovery period, mice were treated intragastrically with Bis-[2-(3,5-dichloropyridyloxy)]benzene (TCPOBOP, 3 mg/kg body weight, Sigma) once/week for 28 weeks. Another group was given only TCPOBOP (once/week) for 42 weeks. The animals were euthanized at 28 and 42 weeks, respectively, time points when HCCs were observed in both the regimen protocols.

Immunohistochemistry

Frozen liver sections were collected and fixed in 10% formalin. Following endogenous peroxidases block (H_2O_2 0.3%, Sigma), aspecific sites were blocked by incubating sections for 30 minutes in 1:10 normal goat serum. Sections were incubated overnight at 4 °C with anti-GSTP antibody (MBL, Nagoya, Japan, MBL, cat# 311, 1:1000) and detected by anti-rabbit HRP (Sigma) and 3-3' diaminobenzidine (Sigma). Sections were counterstained with Harris hematoxylin. For KRT-19 staining, serial sections were fixed in cold acetone for 20 min. Blocking of endogenous peroxidases and aspecific sites was performed as previously described for GSTP staining. Sections were then incubated with primary mouse polyclonal KRT-19 antibody (Novocastra, Wetzlar, Germany, cat# NCL-CK19) at 1:100 dilution overnight at 4 °C and then with anti-mouse HRP and 3,3'-diaminobenzidine.

Laser-capture Microdissection (LMD)

Sixteen µm thick serial frozen sections of rat livers were attached to 2 µm RNase free PEN-membrane slides (Leica, Wetzlar, Germany). Microdissection (Leica, LMD6000) was followed by H&E staining, as described [12]. RNA was extracted from microdissected samples using the PicoPure RNA Isolation Kit (Arcturus, Life Technologies, Carlsbad, CA, USA), according to manufacturer instructions.

Protein extraction and Western blot

For protein analysis, cells and rat liver samples were lysed in 2% SDS, 0.5 M Tris–HCl. Western blots were performed according to standard methods. The following antibodies were used: anti-HAO2 (Santa Cruz Biotechnology, Santa Cruz, CA, USA), and anti–β-actin (I-9, Santa Cruz Biotechnology). Final detection was carried out with the ECL system (Amersham, Uppsala, Sweden).

Cell lines

Human HCC cell lines were cultured in complete medium with 10% fetal bovine serum (Gibco-Life Technologies, Carlsbad, CA) in a 5% CO_2 atmosphere. HepG2 were purchased from ATCC. HA22T/VGH and SKHep1C3.69.2 cells were generously supplied by Dr. G. De Petro [13]; Hep3B-TR, HuH7 and Mahlavu were kindly provided by Dr. N. Atabey; cells were authenticated by genetic sequencing. SNU 182, SNU 398 and SNU 475 were from ATCC (LGC Standards, Milano, Italy). Rat HCC cells (R-H) were isolated by a HCC bearing rat, as described [8].

Evaluation of ROS levels and lipid peroxidation

ROS levels were evaluated using CellRox Green (Thermo Fisher Scientific) following manufacturer's instructions. Fluorescence values were normalized to protein content. Lipid peroxidation was evaluated using TBARS Assay Kit (Cayman Chemical) following manufacturer's instructions. Absorbance values (532 nm) were normalized to protein content. For the detection of total protein redox state, N-(biotinoyl)-N'-(iodoacetyl) ethylene diamine (BIAM) labelling was performed as follows: cells were rapidly rinsed in liquid nitrogen, exposed to RIPA buffer containing 100 µM of BIAM diamine and incubated for 15 min at room temperature. Lysates were then clarified by centrifugation and 500 µg of each sample were immunoprecipitated using 20 µl of Streptavidin-agarose beads (Sigma). Immunocomplexes labelled with BIAM were separated by SDS–PAGE and the biotinylated/reduced fraction was visulalised with conjugated HRP-streptavidin.

Stable transduction with HAO2 and in vivo tumorigenesis experiment

In order to obtain a stable expression, rat R-H cells were transduced either with a lentiviral vector containing the hHAO2 cDNA (pLX304/HAO2, HsCD00439253, DNASU Plasmid Repository Arizona State University, Tempe, AZ) or an empty lentiviral vector as a control (mock). Stably mock and HAO2-transduced R-H cells (1,000,000/mouse) were injected subcutaneously in the flank of CD-1 nude mice (5 mice per group). Tumor size was measured twice a week by caliper. Subcutaneous tumor volume was calculated using the formula 4/3 π (D/2) (d/2) 2, where d is the minor tumor axis and D is the major tumor axis. Mice were sacrificed 19 days after injection, and tumors were excised.

Patients

Two cohorts of patients carrying HCC were examined. In the first, patients' specimens and clinico-pathological data were obtained from the Institute of Pathology, University Hospital of Basel, Switzerland. All patients gave written informed consent to the study, which was approved by the Ethics Committee of the University Hospital of Basel (EKKB). HCC diagnosis was verified by pathological examination; no anticancer treatments were given before biopsy collection. Tumor differentiation was defined according to Edmondson's grading system. Only biopsies containing at least 50% of tumor cells and no necrotic area were used in this study. The clinico-pathologic features of these samples are described in Supplementary Table 1. The second cohort consisted of HCC and cirrothic tissues obtained from 59 consecutive patients (45 males and 14 females, median age ± SD: 65.2 ± 7.9, range 49–80 years) undergoing liver resection for HCC at the Department of Surgery of the University of Bologna. Eight normal liver tissues were obtained from patients undergoing liver surgery for traumatic lesions (5 cases) or haemangioma resection (3 cases). No patient received anticancer treatment prior to surgery. The characteristics of patients are described in Supplementary Table 2. All patients gave written informed consent to the study, which was approved by the Ethics Committee of the University of Bologna.

Human microarray analysis

RNA for the microarray for Transcriptomic profiling was isolated from 59 HCC needle biopsies matched with their corresponding non-neoplastic liver parenchyma and 5 normal liver donors with a Direct-Zol RNA MiniPrep Kit (Zymo Research, Orange, CA, USA) including on-column DNAse treatment. RNA concentration was assessed using Qubit (Invitrogen, Carlsbad, CA, USA) and RNA integrity was monitored on the Bioanalyzer 2100 using the RNA6000 Chip (Agilent, Santa Clara, CA, USA). 270 ng of DNAse-treated total RNA was subjected to target synthesis using the WT Expression kit (Ambion, Austin, TX, USA) following standard recommendations. Fragmentation and labelling of amplified cDNA were performed using the WT Terminal Labelling Kit (Affymetrix, Santa Clara). Synthesis reactions were carried out using a PCR machine (TProfessionnalTrio, Biometra, Göttingen, Germany) in 0.2 ml tubes. 85 µl cocktail (23.4 ng/µl labelled DNA) were loaded on GeneChip®Human Gene 1.0ST arrays (Affymetrix) and hybridized for 17 h (45 °C, 60 rpm) in the Hybridization oven 645 (Affymetrix). The arrays were washed and stained on the Fluidics Stations 450 (Affymetrix) by using the Hybridization Wash and Stain Kit (Affymetrix) under FS450_0002 protocol. The GeneChips were scanned with an Affymetrix GeneChip Scanner 3000 7G. DAT images and CEL files of the microarrays were generated using the Affymetrix GeneChip Command Control (version 4.0). Afterwards, CEL files were imported into Qlucore software and Robust Multichip Average normalized. Subsequently, principal component analysis to discriminate between normal and tumour samples was applied. Quantile normalization and data processing were performed using the GeneSpringGXv11.5.1 software package (Agilent). The gene signature value was assessed using the BRB-ArrayTool (v4.3.2, NIH). Ingenuity software (Qiagen, Hilden, Germany) was used to perform pathways analysis.

qRT-PCR analysis

RNA was retro-transcribed using the High Capacity Kit (Life Technologies). Analysis ofHAO2 was performed using specific TaqMan probes (Life Technologies), and GAPDH as endogenous control. For the second cohort of HCC patients and for the HCC DENA-induced rat model, real-time PCR quantification (IQ SYBR Green Supermix, Bio-Rad

Laboratories, Hercules, CA, USA) of HAO2 was performed by using β-actin as housekeeping gene. Real-Time PCR runs were performed in triplicate. Primers and conditions are listed in Supplementary Table 3.

Statistical analysis

Differences in patient survival were assessed using the Kaplan–Meier method and analysed using the log-rank test in univariate analysis. All tests were two sided and pvalues <0.05 considered statistically significant. Cut-off scores were selected by evaluating the receiver operating characteristic (ROC) curves. The point on the curve with the shortest distance to the coordinate (0, 1) was selected as the threshold value to classify cases as 'positive/overexpressing' or 'negative/downregulated' [14]. Analyses were performed using SPSS software (SPSS Inc, Chicago, IL). For qRT-PCR analyses, data are expressed as mean ± SD or mean ± standard error (SEM). Tests of significance were conducted using Student's t test and one-way ANOVA with post hoc Tukey's test, using GraphPad software (La Jolla, California). Values were considered significant at $p<0.05$.

Results

Hao2 is downregulated all throughout the tumorigenic process in rat liver

The R-H model, which consists of a single injection of the genotoxic agent DENA followed by a short exposure to a promoting environment, allows dissection of the several stages of the carcinogenic process (preneoplastic nodules, adenomas, early HCCs and advanced HCCs) [8] and [15]. Microarray analysis revealed that Hao2 was one of the most downregulated genes in rat advanced HCC (Supplementary Table 4). Since a review of the existing literature did not provide any clue about the role of Hao2 in cancer, we decided to investigate this matter in depth.

With this aim, additional experiments were performed to validate microarray results and, most importantly, to investigate whether Hao2 downregulation is an early event during liver carcinogenesis. Rats were sacrificed at 10 weeks and 14 months after DENA administration, time points at which preneoplastic nodules and HCCs, respectively, are observed. qRT-PCR was then performed on laser-microdissected preneoplastic nodules, identified by their positivity to the neoplastic marker glutathione S-transferase placental form (GSTP) and in HCCs.

As shown in Fig. 1A, qRT-PCR analysis validated the results of our previous microarray data, showing a significant decrease of Hao2 in rat HCC ($p<0.001$). In agreement with mRNA levels, Western blot analysis showed a profound decrease of Hao2 protein (Fig. 1B). Interestingly, a highly significant reduction ($p<0.001$) of Hao2 mRNA levels was observed also in preneoplastic lesions, compared to the liver of control rats (Fig. 1A).

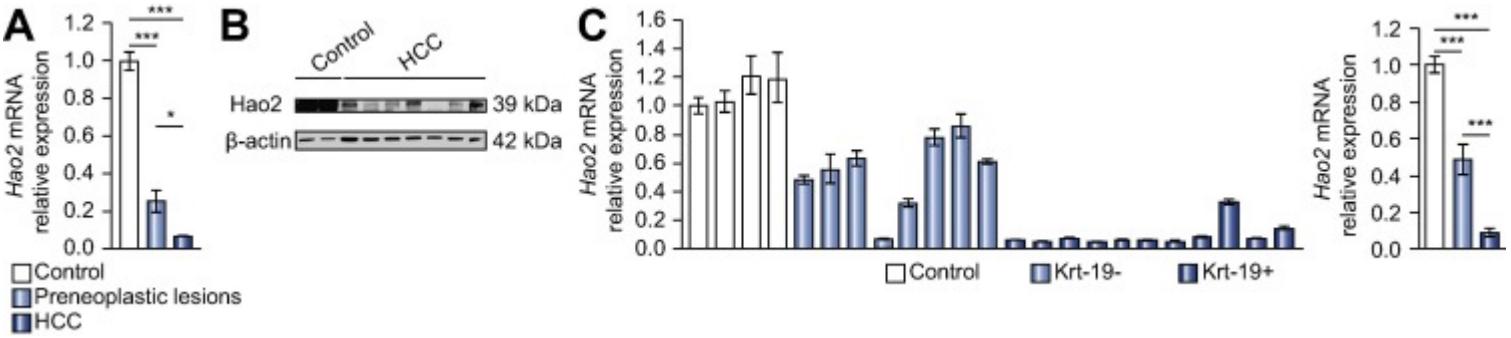

Fig. 1. Hao2 is downregulated in rat preneoplastic nodules and HCCs. (A) Hao2 expression was assessed by quantitative TaqMan RT–PCR in control livers (n = 4), preneoplastic nodules (n = 19) and HCCs (n = 9) developed 10 weeks and 14 months after DENA treatment, using the $2^{-\Delta\Delta Ct}$ method; rat Gapdh was used as endogenous control. Each bar represents mean ± standard error (SEM), calculated as fold change difference; ∗∗∗$p<0.001$, ∗$p<0.05$. (B) Western blot analysis of Hao2 in rat HCC (n = 7) and control liver (n = 2). β-actin was used to normalise protein content. (C) (Left panel) Hao2 mRNA expression in Krt-19$^+$and Krt-19$^-$ lesions obtained 10 weeks after treatment with DENA and controls, calculated as fold change difference; (right panel) average levels of Hao2 expression in the Krt-19$^+$ and Krt-19$^-$ lesions shown in the left panel, calculated as fold change difference compared to

controls. Gapdh was used as endogenous control. Three to four microdissected preneoplastic lesions/animal were examined. Error bars represent SEM; ∗∗∗p <0.001.

Overall, these results suggest that Hao2 downregulation matches the onset of hepatic preneoplastic lesions and accompanies the entire carcinogenic process.

Hao2 is mainly downregulated in the subset of nodules expressing the putative progenitor cell marker Krt-19

In the R-H model, a slow but continuous regression of the vast majority of the preneoplastic lesions occurs through remodeling during the carcinogenic process[16] and [17]. Our previous studies have shown that most HCCs arising in this model are positive for Krt-19, a marker for cholangiocytes, hepatic progenitor cells and early hepatoblasts [18], [19] and [20]. Since in this model, only a minority of preneoplastic lesions developed at early stages of the process are positive for this marker [8] and [15], it is believed that HCCs mainly originate from Krt-19$^+$ preneoplastic lesions. Therefore, we wondered whether downregulation of Hao2 occurs in all preneoplastic populations or is limited to Krt-19$^+$ nodules. To this aim, we microdissected both Krt-19 positive and negative nodules and analysed Hao2 expression. The results showed that althoughHao2 was downregulated in both preneoplastic lesions, the decrease was significantly more pronounced in Krt-19$^+$ than in Krt-19$^-$ nodules ($p < 0.001$) (Fig. 1C). These data indicate that a sustained downregulation of Hao2 expression accompanies the onset and progression of these lesions.

Hao2 downregulation takes place in two other models of rat hepatocarcinogenesis

We next determined the levels of Hao2 mRNA in two other rat models of hepatocarcinogenesis, consisting of; 1) chronic treatment with DENA; and 2) feeding a CMD diet to rats previously injected with a single dose of DENA. In both these protocols HCCs develop in 100% of the animals. The results show that Hao2 is highly significantly downregulated in 12/12 HCCs developed by the CMD protocol and in 16/16 HCCs generated by chronic DENA treatment ($p < 0.0001$) (Supplementary Fig. 1A, B).

Hao2 downregulation is species- and etiology-independent

To determine whether Hao2 downregulation is specific for rat HCC, or, instead, is a more general phenomenon in liver tumorigenesis, we employed a chemically-induced mouse model of hepatocarcinogenesis. This consists of a single injection of DENA followed by treatment with the constitutive androstane receptor (CAR) agonist TCPOBOP that, similar to phenobarbital, causes massive hepatomegaly and leads to HCC in 100% of the mice at 28 weeks after DENA treatment [21]. qRT-PCR analysis of HCCs showed that – similar to the R-H model – Hao2 was strongly downregulated in mouse HCCs, compared to the liver of age-matched control animals ($p < 0.0001$) (Fig. 2A).

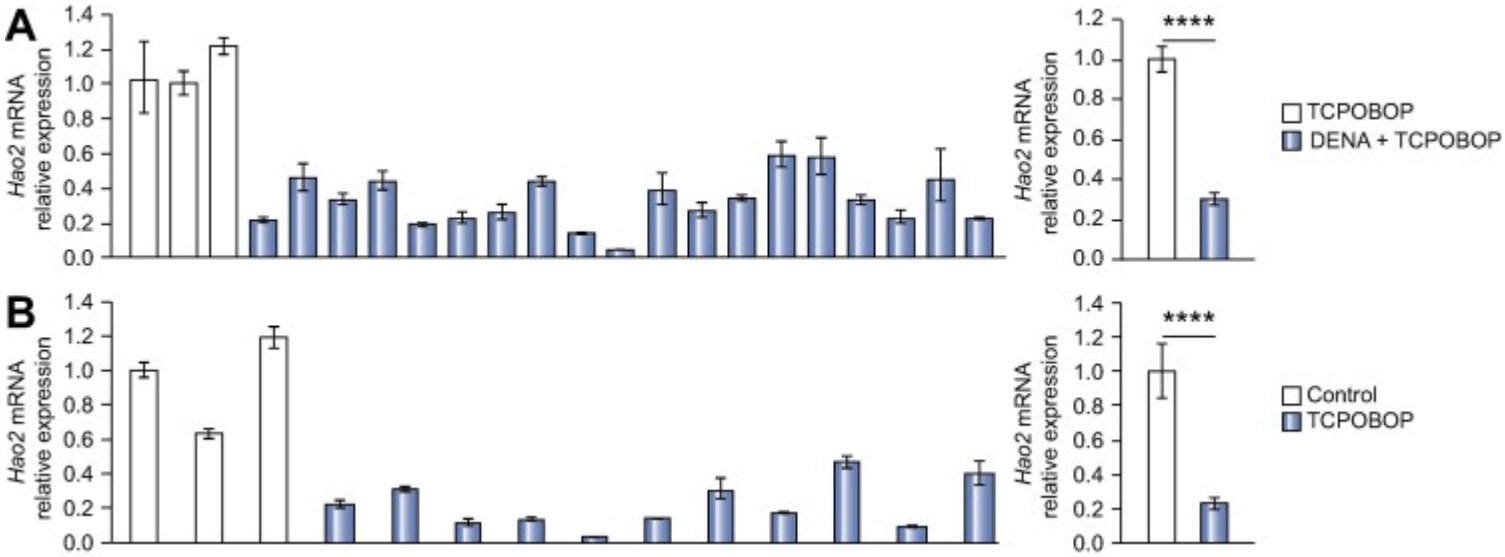

Fig. 2. Hao2 is downregulated in mouse HCCs. (A) (Left panel) Hao2 expression was assessed as described in legend to Fig. 1A in 19 HCCs developed 28 weeks after DENA treatment followed by repeated doses of TCPOBOP and in 3 matched-aged mice treated weekly with TCPOBOP only. Gapdh was used as endogenous control. Error bars represent SEM; (right panel) average levels of Hao2 calculated as fold change difference between HCCs vs. controls shown in the left panel. Error bars represent SEM;

∗∗∗∗p <0.0001. (B) Hao2 expression in 11 HCCs developed 42 weeks after repeated doses of TCPOBOP, in the absence of DENA pre-treatment and 3 control livers. Gapdh was used as endogenous control. Error bars represent SEM; (right panel) average levels of Hao2 calculated as fold change difference between the expression in HCCs vs. controls shown in the left panel. Error bars represent SEM; ∗∗∗∗p <0.0001.

In all the previous models, initiation of the tumorigenic process is triggered by the genotoxic agent DENA. To rule out the possibility that downregulation of Hao2 is the consequence of DNA damage by DENA-derived reactive metabolites, we generated HCCs using a model where liver tumors develop following repeated treatment with the non-genotoxic agent TCPOBOP. Under these conditions, HCCs develop in 100% of the animals, although much later than in the DENA + TCPOBOP group (42 vs. 28 weeks). As shown in Fig. 2B, the expression of Hao2 was strongly inhibited in TCPOBOP (only)-induced HCCs (p <0.0001), demonstrating that Hao2 downregulation is not a consequence of genotoxic treatment.

In human HCCs, HAO2 is downregulated and inversely correlated with tumor grading, metastatic status and overall survival

Next, we assessed whether the results obtained in rodent models could be of translational value for human HCC. Microarray analysis was performed on liver biopsies obtained from patients carrying HCC and healthy liver donors (Supplementary Table 1). The data confirmed HAO2 downregulation in most of the tumors, but not in the surrounding peritumoral tissues (Fig. 3A). Overall, HAO2 was downregulated in 84.7% of HCCs (50 out of 59 tumors), when compared to matched non-cancerous cirrhotic tissues (p <0.01), and in 100% of cases, when compared to normal liver tissues (p <0.0001). Furthermore, lower HAO2 expression was significantly associated to high grade (Edmonson III-IV), more aggressive samples (p <0.05) (Fig. 3B). Stratification of patients according to their etiology did not reveal any significant association with HAO2levels (Fig. 3C). Finally, to explore whether HAO2 expression is associated with clinical progression and outcome of HCC patients, we examined the incidence of metastases and patient overall survival rates using Kaplan-Maier analysis. The metastatic status was defined as either regional lymph node invasion and/or distant organ involvement. LowHAO2 expression correlated with metastasis formation (p <0.05) (Fig. 3D) and decreased overall survival (median 10 and 31 months in low and high HAO2 expressors), respectively (p <0.05) (Fig. 3E).

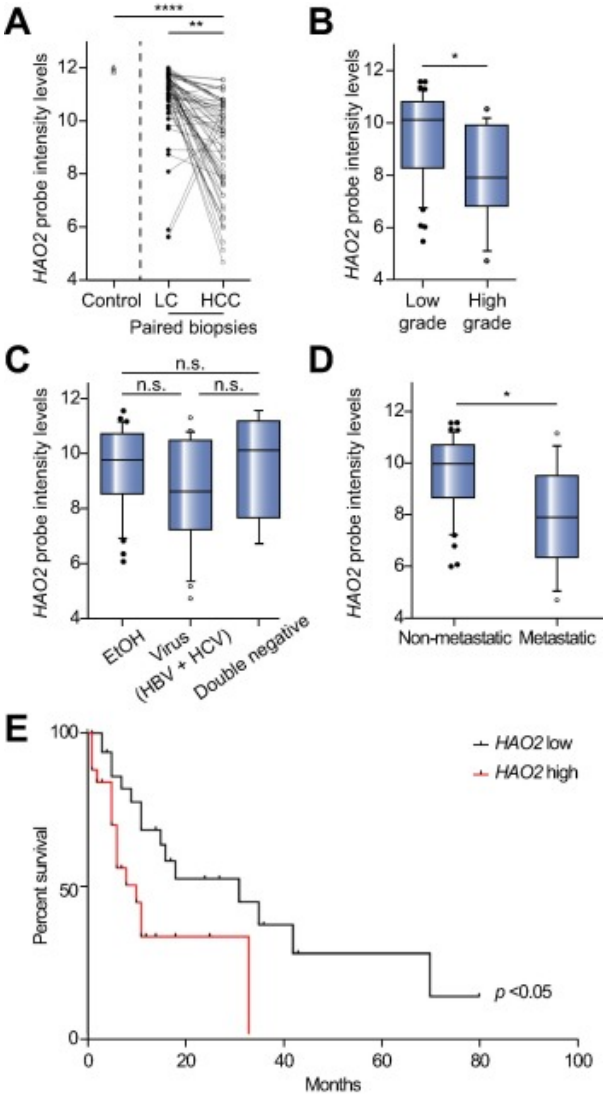

Fig. 3. HAO2 is downregulated in human HCC and inversely correlates with metastatic capacity and overall survival. (A) HAO2 expression in biopsies from human healthy livers (n = 5), HCCs (n = 59) and their peritumoral counterpart (n = 59). HAO2 mRNA levels were assessed by Affimetrix microarray, measured as probe intensity levels and represented as $\log_2$; ∗∗∗∗p <0.0001; ∗∗p <0.01. (B) Stratification of patients according to the Edmondson and Steiner grading system. HAO2 mRNA levels were assessed as described in legend to Fig. 3A. Low (I-II) vs. high grade (III-IV); ∗p <0.05. (C) Stratification of patients according to the etiological agent. HAO2 mRNA levels were assessed as described in legend to Fig. 3A; NS: not significant. (D) HAO2 expression levels in association with metastasis formation. Receiver Operating Characteristic (ROC) curve analysis was used to discriminate between high and low expressing HAO2 levels; ∗p <0.05. (E) HAO2 expression levels in association with overall survival (OS). Survival plot was analysed using the Kaplan–Meier method. ROC curve analysis was used to discriminate between high and low

expressing HAO2 levels; p <0.05. (This figure appears in colour on the web.)

To validate these data, we analysed HAO2 mRNA levels in a confirmatory cohort of 59 human HCCs (the characteristics of the study population are described in Supplementary Table 2) and their corresponding peritumoral tissues. Similarly to what was observed in the previous cohort, HCCs showed a significant downregulation of HAO2 mRNA compared to matched cirrhotic tissues (Liver Cirrhosis (LC)), as well as to normal liver (Fig. 4A). Indeed, qRT-PCR analysis revealed that HAO2 was downregulated in HCC tissues when compared to both LC tissues (p <0.0001) and to normal liver tissues (p <0.0001). Overall, HAO2 was downregulated in 88% of HCCs, when compared to matched non-cancerous cirrhotic tissues, and in 92% of cases, when compared to normal liver tissues (Fig. 4B). Also in this cohort, no HAO2 decrease was observed in the cirrhotic tissue compared to normal liver tissue. In agreement with the mRNA levels, Western blot analysis showed a decreased HAO2 protein content in 6/7 HCCs examined, compared to their corresponding cirrhotic tissues (Fig. 4C).

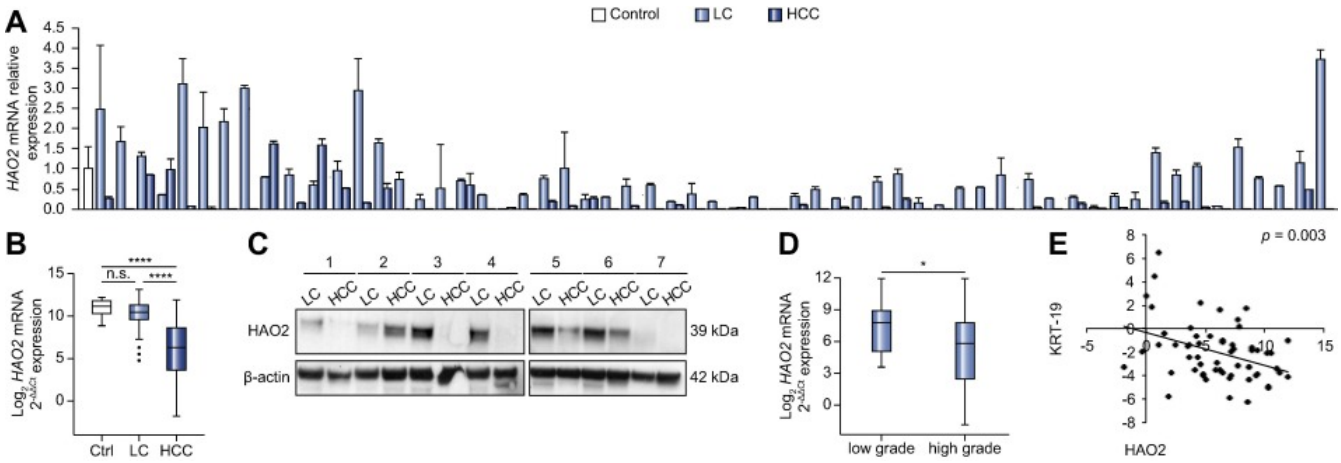

Fig. 4. HAO2 is downregulated in a validation setting of resected human HCCs. (A) HAO2 expression in human resected HCCs (n = 59) and their peritumoural cirrhotic liver (liver cirrhosis (LC); n = 59). Relative levels of HAO2 mRNA in HCC and LC samples were calculated with respect to the mean value of HAO2mRNA expression of 8 normal livers. Error bars represent SD; β-actin was used as endogenous control. (B) Box-plot graphic representation of HAO2 mRNA levels in HCCs, LCs and normal livers shown inFig. 4A. The y-axis represents $2^{-\Delta\Delta Ct}$ values in a $\log_2$ form; ∗∗∗∗p <0.0001; n.s.: not significant. (C) Western blot analysis of HAO2 in 7 HCCs and matched peritumoural tissues. β-actin was used to normalise protein content. (D) Box-plot graphic representation of HAO2 mRNA levels in HCC samples grouped according to Edmondson and Steiner grading score. Low grade HCCs: I and II; high grade HCCs: III and IV. The y-axis represents $2^{-\Delta\Delta Ct}$ values in a $\log_2$ form; ∗p <0.05. (E) Graphic representation showing an inverse relationship between HAO2 and KRT-19 mRNA levels in human resected HCCs;p = 0.003.

The expression of HAO2 was significantly lower in high grade (mean 7.51 ± 2.76) vs. low grade tumors (mean 5.36 ± 3.51; p <0.05; Fig. 4D). Stratification of patients according to the etiology of the underlying liver disease, as well as tumor size, did not reveal any significant association with HAO2 expression in tumor tissue (not shown). Interestingly, in agreement with the rat model, an inverse relationship between HAO2 and KRT-19mRNA levels was observed in human resected HCCs (Fig. 4E).

Altogether these data show that in humans, as well as in rodents, HAO2 expression is significantly decreased during HCC progression. Moreover, this decrease correlates with poor prognosis.

Exogenous expression of Hao2 impairs the tumorigenic capacity of rat HCC cells in vivo

To gain a better understanding of the biological role of HAO2 we moved to in vitro studies. With this aim, we determined HAO2 expression in human HCC cell lines. qRT-PCR analysis showed that all the cell lines examined expressed very low or undetectable levels of HAO2 mRNA (C_t ranging from 32-34 in HuH7 and HepG2, to 37-39 in all the other cell lines); (Supplementary Fig. 2). Accordingly, no detectable signal was observed in Western blot (Fig. 5A). Low Hao2 expression was also found in R-H rat liver cells obtained from a HCC bearing rat [8] (Fig. 5B).

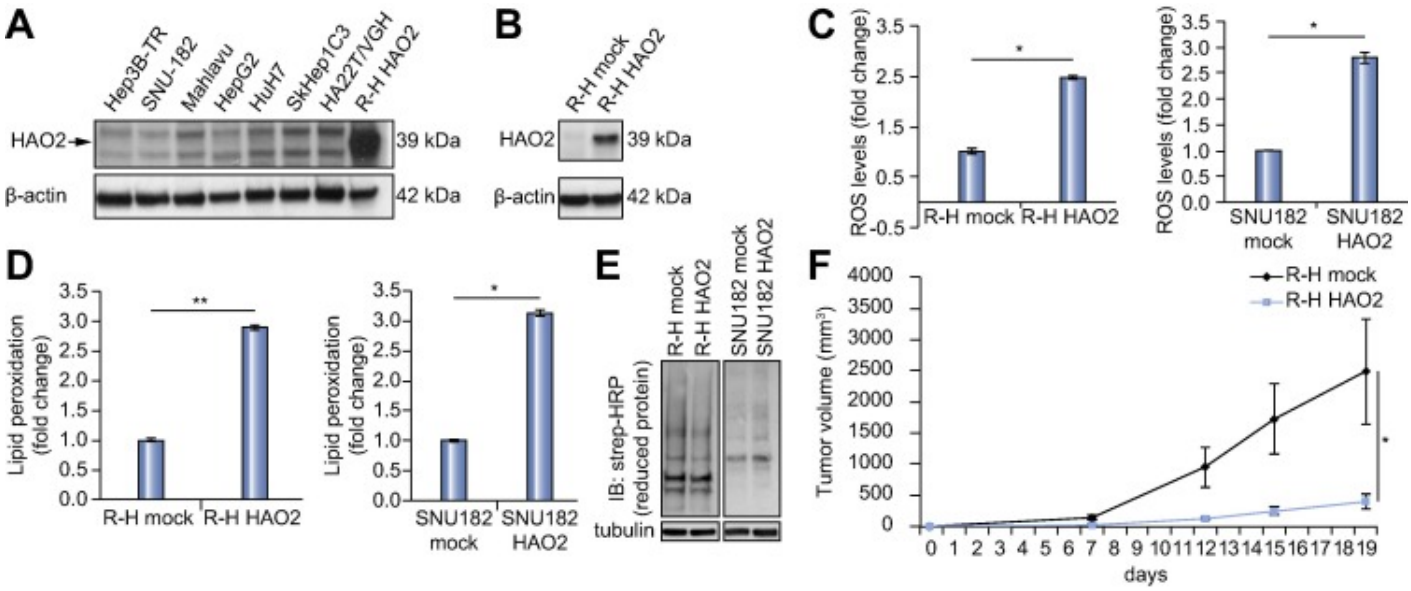

Fig. 5. Transduction of HAO2 impairs the tumorigenic ability of rat HCC cells. (A) Western blot analysis of HAO2 protein content in human HCC cell lines. HAO2-transduced R-H rat cells were used as positive control. (B) Western blot analysis of R-H cells transduced with a lentiviral vector containing HAO2 cDNA or an empty vector (mock). β-actin was used to normalise protein content. (C) HAO2 expression enhanced ROS levels in both rat R-H (left) and human SNU182 (right) HCC cell lines. Bars represents mean ± SEM (n = 3). One-way ANOVA; Dunnett's corrected; ∗p <0.05, ∗∗p <0.01; (D) Enhanced ROS levels induced by HAO2 overexpression increased lipid peroxidation in both HCC R-H cells (left) and the human SNU182 HCC cell line (right). Bars represent mean ± SEM (n = 3). One-way ANOVA; Dunnett's corrected; ∗p <0.05, ∗∗∗p <0.001. (E) Total levels of reduced proteins were not affected by HAO2 overexpression, as measured with BIAM labelling (see materials and methods). (F) 1×10^6 R-H cells transduced with empty vector (R-H mock) or with HAO2 cDNA (R-H HAO2) were subcutaneously injected into the right posterior flanks of CD-1 nude mice. The graph shows tumor size, evaluated twice weekly by caliper; approximate volume of the mass was calculated as indicated in materials and methods. Bars represent the mean ± SEM (n = 5), student's t test; ∗p <0.05.

To establish whether the enzymatic activity of HAO2 might increase the levels of reactive oxygen species (ROS) and, consequently, play a role in cell injury, we determined the levels of ROS and lipid peroxidation in wild-type and HAO2-transduced R-H and human cell lines. As shown in Fig. 5C, D, HAO2 transduction in both human and rat HCC cells led to enhanced ROS levels and to increased lipid peroxidation, further supporting the hypothesis that the reduced levels of HAO2 in HCC might contribute to a better survival of cancer cells. No significant difference of protein peroxidation was observed, as expected for a lipid peroxidase such as HAO2 (Fig. 5E).

To evaluate the oncosuppressive role of HAO2 in HCC cells, we transduced rat R-H cells with a lentiviral construct containing hHAO2 cDNA. HAO2 exogenous expression significantly impaired HCC cells tumorigenic ability; indeed, when subcutaneously grafted into immunodepressed mice, R-H cells transduced with an empty vector (mock) were able to form HCCs in all animals, while tumor growth was significantly impaired in mice subcutaneously injected with HAO2-transduced cells (Fig. 5F; Supplementary Fig. 3). These experiments suggest that HAO2 acts as an oncosuppressor in HCC cells.

Discussion

L-2-Hydroxy acid oxidases are responsible for the oxidation of a number of L-2-hydroxy acids to ketoacids resulting in the formation of hydrogen peroxide [1] and thus in increased ROS levels which, in turn, may either lead to cell injury, or stimulate cell proliferation [6] and [7]. Since no data are available concerning the role of HAO2 in cancer, we investigated its role in the onset and development of HCC.

The main findings stemming from our work indicate that downregulation of HAO2, i) occurs in HCC developed in different models of hepatocarcinogenesis and in three different species (100% of rat and mouse HCCs and 70–80% of human

HCCs); ii) is etiology-independent; iii) represents a very early event in the multistage process of hepatocarcinogenesis; and iv) correlates with poor prognosis in humans.

Altogether, these results demonstrate that HAO2 downregulation is associated with HCC onset and progression, in a species- and etiology-independent fashion. Furthermore, these results suggest that HAO2 acts as a tumor suppressor gene. Indeed, HAO2transduction in HCC cells impaired tumorigenic ability in vivo.

At the moment, no data are available to explain HAO2 loss. Mechanisms such as epigenetic or genetic alterations and post-transcriptional regulation, like that caused by miRNAs, could be involved. Searching for HAO2-targeting miRNAs, we found that HAO2contains miR-183 binding sites on its 3'-UTR. Notably, this miRNA was found to be upregulated in Krt-19 positive preneoplastic lesions and HCCs (74- and 14-fold, respectively) [8], and exhibiting HAO2 downregulation vs. control liver. Further studies are required to establish if this or other miRNAs are indeed involved in HAO2downregulation.

Although at present it is unclear why loss of HAO2 influences hepatocarcinogenesis, we can speculate that this enzyme plays a role in hepatocyte proliferation. Indeed, the findings that i) maximal Hao2 downregulation occurs in the most aggressive rat preneoplastic lesions (Krt-19^{+}), which proliferate at a much higher rate than those negative for this marker, and that ii) it is significantly associated with poorly differentiated HCCs (Edmondson III-IV), suggest that loss of this gene plays a relevant role in the evolution of preneoplastic lesions and in the progression of malignant HCC cells. Of note, similar data were obtained from two different cohorts of patients and two different types of tissue specimens, namely surgical liver resections and needle liver biopsies. Moreover, snap-frozen needle biopsies and surgical resections were collected from patients who did not receive any HCC-tailored therapeutic treatment prior to the biopsy. In both the groups, HAO2 downregulation correlated with low tumor grade, and in the evaluation cohort (where it was possible to evaluate the patient's follow-up) HAO2 downregulation correlated with increased metastatic ability and decreased overall survival. A possible explanation for the biological effect driven by loss of HAO2 could be linked to the ability of this enzyme to produce hydrogen peroxide. As shown by our data, increased expression of HAO2 resulted in increased ROS production and lipid peroxidation. Loss of this enzyme may thus represent a cytoprotective mechanism by which genetically-altered cells can escape excessive ROS generation and cell damage.

Search for genes/proteins whose expression can discriminate between normal and neoplastic liver and, most importantly, between cirrhotic and neoplastic lesions is fundamental for prognostic and diagnostic purposes. Therefore, the observation thatHAO2 expression is virtually absent in preneoplastic/dysplastic lesions is novel and very interesting from a diagnostic point of view. Indeed, the finding that cirrhotic areas in humans are positive for HAO2 could allow early identification of dysplastic nodules and their discrimination from cirrhotic regenerative nodules. Since the availability of markers able to differentiate these two lesions represents a still unsolved problem in human pathology, our data suggest that HAO2 should be evaluated as such a marker. Moreover, as its loss strongly correlates with a poor outcome, it is conceivable that HAO2 could be associated with other markers known to share a negative prognostic value, in order to personalize therapy in HCC patients.

Financial support

This work was supported by Associazione Italiana Ricerca sul Cancro (AIRC – Italy, Grants IG-15279 to AC and IG-15464 to SG), Ministero Università e Ricerca Scientifica(PRIN-2010LC747T to AC), R.A.S. – Italy 2012 to AC and Fondazione Banco di Sardegna – Italy to AC, GMLC and APerra. SM is an AIRC fellow.

Conflict of interest

The authors who have taken part in this study declared that they do not have anything to disclose regarding funding or conflict of interest with respect to this manuscript.

Authors' contributions

Conception and design: SM, AP, SG, AC; Provision of study materials or patients: SM, MMA, APe, LT, LQ, LG, FF; Acquisition of data: SM, AP, GMLC, SMe, LG, APe, PC, AM, AM; Analysis and interpretation of data: SM, AP, GMLC,

SMe, PC, AM, SG, AC; Writing, review, and/or revision of the manuscript: SM, GMLC, LT, PC, LG, SG,AC; Study supervision: AC, SG.

References

[1] J.M. Jones, J.C. Morrell, S.J. Gould. Identification and characterization of HAOX1, HAOX2, and HAOX3, three human peroxisomal 2-hydroxy acid oxidases. J Biol Chem, 275 (2000), pp. 12590–12597

[2] D.A. Barawkar, A. Bandyopadhyay, A. Deshpande, S. Koul, S. Kandalkar, P. Patil, et al. Discovery of pyrazole carboxylic acids as potent inhibitors of rat long chain L-2-hydroxy acid oxidase. Bioorg Med Chem Lett, 22 (2012), pp. 4341–4347

[3] S. Angermüller. Peroxisomal oxidases: cytochemical localization and biological relevance. Prog Histochem Cytochem, 20 (1989), pp. 1–65

[4] D.W. Fry, K.E. Richardson. Isolation and characterization of glycolic acid oxidase from human liver. Biochim Biophys Acta, 568 (1979), pp. 135–144

[5] H. Schwam, S. Michelson, W.C. Randall, J.M. Sondey, R. Hirschmann. Purification and characterization of human liver glycolate oxidase. Molecular weight, subunit, and kinetic properties. Biochemistry, 18 (1979), pp. 2828–2833

[6] D. Trachootham, W. Lu, M.A. Ogasawara, R.D. Nilsa, P. Huang Redox regulation of cell survival. Antioxid Redox Signal, 10 (2008), pp. 1343–1374

[7] J.M. Matés, J.A. Segura, F.J. Alonso, J. Márquez. Intracellular redox status and oxidative stress: implications for cell proliferation, apoptosis, and carcinogenesis. Arch Toxicol, 82 (2008), pp. 273–299

[8] A. Petrelli, A. Perra, D. Cora, P. Sulas, S. Menegon, C. Manca, et al. MicroRNA/gene profiling unveils early molecular changes and nuclear factor erythroid related factor 2 (NRF2) activation in a rat model recapitulating human hepatocellular carcinoma (HCC). Hepatology, 59 (2014), pp. 228–241

[9] D.B. Solt, A. Medline, E. Farber. Rapid emergence of carcinogen-induced hyperplastic lesions in a new model for the sequential analysis of liver carcinogenesis. Am J Pathol, 88 (1977), pp. 595–618

[10] H. Shinozuka, B. Lombardi, S. Sell, R.M. Iammarino. Early histological and functional alterations of ethionine liver carcinogenesis in rats fed a choline-deficient diet. Cancer Res, 38 (1978), pp. 1092–1098

[11] M.F. Rajewsky, W. Dauber, H. Frankenberg. Liver carcinogenesis by diethylnitrosamine in the rat. Science, 152 (1996), pp. 83–85

[12] A. Perra, M.A. Kowalik, E. Ghiso, G.M. Ledda-Columbano, L. Di Tommaso, M.M. Angioni, et al.. YAP activation is an early event and a potential therapeutic target in liver cancer development. J Hepatol, 61 (2014), pp. 1088–1096

[13] A. Salvi, C. Sabelli, S. Moncini, M. Venturin, B. Arici, P. Riva, et al.. MicroRNA-23b mediates urokinase and c-met downmodulation and a decreased migration of human hepatocellular carcinoma cells. FEBS J, 276 (2009), pp. 2966–2982

[14] S. Piscuoglio, F.S. Lehmann, I. Zlobec, L. Tornillo, W. Dietmaier, A. Hartmann, et al. Effect of EpCAM, CD44, CD133 and CD166 expression on patient survival in tumours of the ampulla of Vater. J Clin Pathol, 65 (2012), pp. 140–145

[15] J.B. Andersen, R. Loi, A. Perra, V.M. Factor, G.M. Ledda-Columbano, A. Columbano, et al.. Progenitor-derived hepatocellular carcinoma model in the rat. Hepatology, 51 (2010), pp. 1401–1409

[16] K. Enomoto, E. Farber. Kinetics of phenotypic maturation of remodeling of hyperplastic nodules during liver carcinogenesis. Cancer Res, 42 (1982), pp. 2330–2335

[17] A. Perra, M.A. Kowalik, M. Pibiri, G.M. Ledda-Columbano, A. Columbano. Thyroid hormone receptor ligands induce regression of rat preneoplastic liver lesions causing their reversion to a differentiated phenotype. Hepatology, 49 (2009), pp. 1287–1296

[18] A. Durnez, C. Verslype, F. Nevens, J. Fevery, R. Aerts, J. Pirenne, et al..The clinicopathological and prognostic relevance of cytokeratin 7 and 19 expression in hepatocellular carcinoma. A possible progenitor cell origin. Histopathology, 49 (2006), pp. 138–151

[19] J.S. Lee, J. Heo, L. Libbrecht, I.S. Chu, P. Kaposi-Novak, D.F. Calvisi, et al. A novel prognostic subtype of human hepatocellular carcinoma derived from hepatic progenitor cells. Nat Med, 12 (2006), pp. 410–416

[20] L. Libbrecht, V. Desmet, B. Van Damme, T. Roskams. The immunohistochemical phenotype of dysplastic foci in human liver: correlation with putative progenitor cells. J Hepatol, 33 (2000), pp. 76–84

[21] M.A. Kowalik, C. Saliba, M. Pibiri, A. Perra, G.M. Ledda-Columbano, I. Sarotto, et al. Yes-associated protein regulation of adaptive liver enlargement and hepatocellular carcinoma development in mice. Hepatology, 53 (2011), pp. 2086–2096

Corresponding authors. Address: Department of Oncology, University of Torino, Medical School, Candiolo Cancer Institute-FPO, IRCCS, Strada, Provinciale 142, Candiolo (Torino) 10060, Italy. Tel.: +39 0119933233; fax: +39 0119933225 (S. Giordano), or Department of Biomedical Sciences, Unit of Oncology and Molecular Pathology, University of Cagliari, Via Porcell 4, 09124 Cagliari, Italy. Tel.: +39 0706758345; fax: +39 070666062 (A. Columbano).